

From prelife to life: a bio-inspired toy model

H.J. Hilhorst

Laboratoire de Physique Théorique, UMR 8627
Université Paris-Sud and CNRS
Bâtiment 210, 91405 Orsay Cedex, France

December 24, 2021

Abstract

We study a one-dimensional lattice of N sites each occupied by a mathematical “polymer,” that is, is a binary random sequence of arbitrary length n , or equivalently, a rooted path of n links on an infinite binary tree. The average polymer length is controlled by the monomer fugacity z . A pair of polymers on adjacent sites carries a weight factor ω for each link on the tree that they have in common. The phase diagram in the $z\omega$ plane exhibits a critical line $z = z_c(\omega)$. For $z < z_c(\omega)$ there exists an equilibrium phase with, in particular, a finite average polymer length. We investigate the equilibrium ensemble by transfer matrix and Monte Carlo methods, paying particular attention to the vicinity of the critical line. For $z > z_c(\omega)$ the equilibrium is unstable and Monte Carlo time evolution brings about a dynamical symmetry breaking which favors the evolution of a small selection of polymers to ever greater length. While of interest for its own sake, this model may also be relevant to the prelife-to-life transition that has occurred during biological evolution. We compare it to existing models of similar simplicity due to Wu and Higgs (2009, 2012) and to Chen and Nowak (2012).

Keywords: phase transitions; evolution of species; prelife-to-life transition; artificial chemistry.

1 Introduction

Explaining the appearance of life in the prebiotic soup billions of years ago is an intriguing but extremely difficult question. It involves the statistics as well as the physics, chemistry, and biology of interacting macromolecules. Mathematical models of this prelife-to-life transition, whether simple or more elaborate, can never do justice to the full complexity of the problem, but at most shed some light on certain aspects of it. In this work we present and discuss a model altogether at the simplistic end of the spectrum. It may be characterized as a bio-inspired toy model designed for statistical physicists.

An early statistical model describing the transition from prelife to life was formulated by Dyson [1] decades ago. At its core there is a bistable Fokker-Planck equation governing the fraction of monomers that are “active,” *i.e.* that participate in autocatalytic processes in the system. The stationary states with the lower and higher fraction of active monomers are interpreted as prebiotic and alive, respectively. Dyson’s solution amounts to an application of Kramers’ escape rate theory [2].

Models of similar kind and almost equal simplicity were studied by Wu and Higgs [3, 4] and by Chen and Nowak [5]. Wu and Higgs [3] consider a set of coupled rate equations for the concentrations of polymers of given lengths, without regard for their specific monomer sequence. Chen and Nowak model a reservoir of two types of monomers from which an arbitrary number of polymer species may grow, each species being determined by its length and its monomer sequence. In all these models “life” is identified with the appearance of an autocatalytic feedback that arises once there is an appreciable concentration of sufficiently long polymers.

The merits of such models, notwithstanding the gross simplifications upon which they rely, have been emphasized by workers in the field of mathematical biology [6] and artificial chemistry [7]. Dyson minimizes the pretensions of his work by stating that it is “not intended to be a theory of the origin of life”; but stresses that such models may help to ask new questions.

In this work we describe a mixture of species at the level of individual polymers which are composed of two types of monomers. Only two parameters play a role, namely the monomer fugacity z and a weight factor ω representing an interaction between polymers. In the $z\omega$ plane there is a parameter regime corresponding to an equilibrium state (the prebiotic soup) and another parameter regime (the state sustaining life) in which the system is unstable and forms ever longer polymers. The model shows in particular the possibility of the emergence of a single or a few dominant polymer species. Much of this work concentrates on the transition between the two regimes.

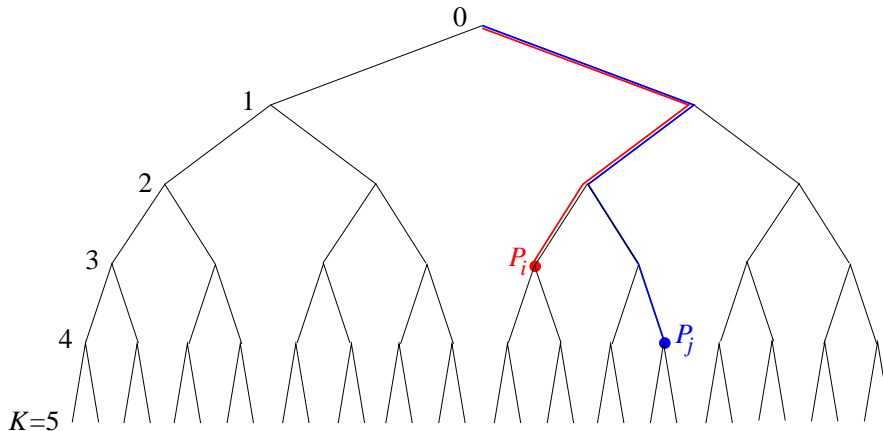


Figure 1: A rooted binary tree of depth $K = 5$. The two rooted paths P_i (red) and P_j (blue) have lengths 3 and 4, respectively. They have their first two links in common and hence have an overlap $\ell_{ij} = 2$. A rooted path is also called a “polymer,” and its links “monomers.”

In section 2 we define the model. In section 3 we study its equilibrium state by a combination of heuristic arguments, Monte Carlo simulation, and analytic work using the transfer matrix. In section 4 we investigate the unstable regime by means of heuristic arguments and Monte Carlo simulation. In our discussion in section 5 we elaborate, in particular, upon the similarities and the differences between this work and that of references [3]-[5]. In section 6 we conclude briefly.

2 Model

Let a one-dimensional lattice have sites $i = 1, 2, \dots, N$. On each site i lives a mathematical “polymer” P_i . The monomers composing the polymer may be of two different types, denoted by $+1$ and -1 . We write the polymer variable as $P_i = (n_i; p_i^{n_i})$ in which n_i is the number of monomers in P_i and where $p_i^{n_i} \equiv (s_{i1}, s_{i2}, \dots, s_{i,n_i})$, with monomer variables $s_{ik} = \pm 1$, gives the detailed monomer structure of P_i .

Each polymer P_i may be represented by a rooted path (that is, a path starting from the origin) on a binary tree (see figure 1), under the convention that a link going down to the left (down to the right) corresponds to a monomer of type -1 (of type $+1$). We allow the polymer length n_i to take the values $0, 1, 2, \dots, K$, with $n_i = 0$ standing for the absence of a polymer on site i , and where K is a cutoff length that we will send to infinity at a later stage.

By the *overlap* ℓ_{ij} between two paths P_i and P_j we will mean the number of links on the tree that they have in common. As is clear from figure 1, when the k th link is not in common, then the links of indices higher than k , if any, cannot be in common either.¹ We will also use the more explicit notation $\ell_{ij} \equiv \ell(p_i^{n_i}, p_j^{n_j})$.

Let $P \equiv (P_1, P_2, \dots, P_N)$ be a system configuration. We associate with it an *energy* $E[P]$ that depends on two parameters, namely the monomer chemical potential μ and the overlap energy $-\epsilon$. Explicitly, we set

$$E[P] = -\mu \sum_{i=1}^N n_i - \epsilon \sum_{i=1}^{N-1} \ell_{i,i+1}. \quad (2.1)$$

The second term on the RHS of (2.1) is one of the simplest ways to introduce a polymer-polymer interaction. It expresses that in order for one long polymer to catalytically favor the growth of another one, their two monomer sequences have to be in a precise relation. We note that this second term corresponds to free boundary conditions.

Let β stand for the inverse temperature. We will employ two alternative variables, the monomer fugacity z and the “overlap weight” ω , defined as

$$z = e^{\beta\mu}, \quad \omega = e^{\beta\epsilon}, \quad (2.2)$$

in terms of which the Boltzmann weight of a configuration P becomes

$$e^{-\beta E[P]} = z^{\sum_{i=1}^N n_i} \omega^{\sum_{i=1}^{N-1} \ell_{i,i+1}}. \quad (2.3)$$

We will restrict ourselves to $\epsilon > 0$, or equivalently to an overlap weight $\omega > 1$, which favors overlap between neighboring polymers, the case $\omega = 1$ being the trivial interactionless limit.

We will find that in the $z\omega$ plane there is an equilibrium regime (to be called regime I) where the equilibrium properties of this model are well-defined in the limit of an infinite cutoff, $K \rightarrow \infty$. This regime is studied in section 3.1. In the remaining regimes (to be called IIa, IIb, and III) there is, for infinite cutoff, no equilibrium state and a dynamic description becomes necessary. To that end we have endowed this model with a standard heat bath Monte Carlo dynamics. The algorithm allows each polymer P_i to change its length by addition or suppression of a single monomer at a time, supposedly due to an exchange with a reservoir of monomers of the two types.

¹ The overlap between P_i and P_j is formally given, therefore, by $\ell_{ij} = \sum_{k=1}^{\min(n_i, n_j)} \prod_{k'=1}^k \frac{1}{2}(1 + s_{ik'} s_{jk'})$, but this expression will not be of help in practice.

3 Equilibrium

3.1 Reduced transfer matrix

In the equilibrium regime, whose exact location in the $z\omega$ plane has yet to be determined, the thermodynamic properties of the system follow from its partition function

$$Z_N(z, \omega) = \sum_P e^{-\beta E[P]}. \quad (3.1)$$

In terms of Z_N the average polymer length $\langle n \rangle$ and the average overlap $\langle \ell \rangle$ between neighboring polymers are given by

$$\langle n \rangle = \frac{1}{N} \frac{\partial \log Z_N}{\partial \log z}, \quad \langle \ell \rangle = \frac{1}{N-1} \frac{\partial \log Z_N}{\partial \log \omega}. \quad (3.2)$$

The calculation of Z_N may be formulated as a transfer matrix problem. The number \mathcal{K} of states accessible to the variable P_i equals $\mathcal{K} = \sum_{n_i=0}^K 2^{n_i} = 2^{K+1} - 1$, which would lead to a $\mathcal{K} \times \mathcal{K}$ transfer matrix. We will show now that it is possible at a set of fixed polymer lengths $\{n_i\}$ to analytically sum over the polymer configurations $\{p_i^{n_i}\}$, which then leaves us with a drastically reduced transfer matrix of size $(K+1) \times (K+1)$.

Using that $\sum_P = \prod_i \sum_{P_i} = \prod_i \sum_{n_i} \sum_{p_i^{n_i}}$ we have from (3.1) and (2.3), after suitably arranging the factors,

$$\begin{aligned} Z_N(z, \omega) = & \sum_{n_1} z^{n_1} \sum_{p_1^{n_1}} \sum_{n_2} z^{n_2} \sum_{p_2^{n_2}} \omega^{\ell(p_1^{n_1}, p_2^{n_2})} \sum_{n_3} z^{n_3} \sum_{p_3^{n_3}} \omega^{\ell(p_2^{n_2}, p_3^{n_3})} \dots \\ & \dots \sum_{n_N} z^{n_N} \sum_{p_N^{n_N}} \omega^{\ell(p_{N-1}^{n_{N-1}}, p_N^{n_N})}. \end{aligned} \quad (3.3)$$

Because of the free boundary conditions there are no factors of ω due to overlap of $p_1^{n_1}$ and $p_N^{n_N}$. We will now show that the sums on $p_N^{n_N}, p_{N-1}^{n_{N-1}}, \dots, p_2^{n_2}$ in expression (3.3) may be carried out successively in that order. The sum on $p_N^{n_N}$, which involves 2^{n_N} terms, may be rewritten as

$$T_{n_{N-1}, n_N} \equiv \sum_{p_N^{n_N}} \omega^{\ell(p_{N-1}^{n_{N-1}}, p_N^{n_N})} = \sum_{\ell=0}^{\min(n_{N-1}, n_N)} g_{n_{N-1} n_N}(\ell) \omega^\ell, \quad (3.4)$$

in which $g_{nm}(\ell)$ is the number of configurations of a polymer of length m to have an overlap exactly equal to ℓ with a given polymer of length n . An elementary calculation with the abbreviation $\nu = \min(m, n)$ leads to

$$g_{nm}(\ell) = 2^{\max(m-n, 0)} \times \begin{cases} 2^{\nu-\ell-1} & 0 \leq \ell \leq \nu - 1, \\ 1 & \ell = \nu, \end{cases} \quad (3.5)$$

valid for $0 \leq n, m \leq K$. It is easily verified that $\sum_{\ell=0}^m g_{nm}(\ell) = 2^m$, which is the total number of configurations of the polymer of length m , as it had to be. Substituting (3.5) in (3.4) and carrying out the sum on ℓ yields

$$T_{nm} = 2^{\max(m-n, 0)} f(\nu), \quad f(\nu) = \begin{cases} 1, & \nu = 0, \\ \frac{\omega^\nu - 2^\nu}{\omega - 2} + \omega^\nu, & \nu = 1, 2, \dots, K, \end{cases} \quad (3.6)$$

valid for $\omega \neq 2$ (we will leave the special case $\omega = 2$ aside).

Since the result of this summation depends on n_{N-1} but not on $p_{N-1}^{n_{N-1}}$, we can now repeat the procedure and carry out the sum on $p_{N-1}^{n_{N-1}}$ at fixed path length n_{N-1} . Working our way down through the chain and still using that the final sum on $p_1^{n_1}$ just yields a factor 2^{n_1} we get

$$Z_N(z, \omega) = \sum_{n_1} \sum_{n_2} \dots \sum_{n_N} 2^{n_1} z^{n_1+n_2+\dots+n_N} T_{n_1, n_2} T_{n_2, n_3} \dots T_{n_{N-1}, n_N}. \quad (3.7)$$

In terms of the symmetric matrix

$$\tilde{T}_{nm} = (2z)^{\frac{n}{2}} T_{nm} \left(\frac{z}{2}\right)^{\frac{m}{2}} = 2^{|n-m|/2} z^{(n+m)/2} f(\nu) \quad (3.8)$$

the partition function (3.7) becomes

$$Z_N(z, \omega) = \sum_{n=0}^K \sum_{m=0}^K (2z)^{\frac{n+m}{2}} (\tilde{T}^{N-1})_{nm}. \quad (3.9)$$

This achieves expressing Z_N in terms of a transfer matrix of the reduced size $K+1$.

Let $\lambda_0 \geq \lambda_1 \geq \dots \geq \lambda_K$ be the set of eigenvalues of \tilde{T} and let $\psi^{(k)}$ be the normalized eigenvector with eigenvalue λ_k , so that we have the decomposition

$$\tilde{T}_{nm} = \sum_{k=0}^K \psi_n^{(k)} \lambda_k \psi_m^{(k)}. \quad (3.10)$$

Substitution of (3.10) in (3.9) yields

$$Z_N(z, \omega) = \sum_{k=0}^K \left| \sum_{m=0}^K (2z)^{\frac{m}{2}} \psi_m^{(k)} \right|^2 \lambda_k^{N-1} \quad (3.11)$$

whence in the limit of large system size

$$\log Z_N(z, \omega) = N \log \lambda_0 + \mathcal{O}(N^0), \quad N \rightarrow \infty, \quad (3.12)$$

and therefore, with equations (3.2),

$$\langle n \rangle = \frac{\partial \log \lambda_0}{\partial \log z} + \mathcal{O}(N^{-1}), \quad \langle \ell \rangle = \frac{\partial \log \lambda_0}{\partial \log \omega} + \mathcal{O}(N^{-1}), \quad N \rightarrow \infty. \quad (3.13)$$

We now refine the preceding analysis. Let $Z_N^{(n,j)}(z, \omega)$ be the expression identical to (3.7) except for the insertion of an extra factor δ_{n,n_j} in the inner summand; the ratio $Z_N^{(n,j)}(z, \omega)/Z_N(z, \omega) \equiv \mathcal{P}_N^{(j)}(n)$ is then the probability that the polymer at site j be exactly of length n . Upon taking $Z_N^{(n,j)}(z, \omega)$ through the same procedure as we did for $Z_N(z, \omega)$ we find that in the large N limit and for j sufficiently deep in the bulk, one has $Z_N^{(n,j)}(z, \omega)/Z_N(z, \omega) \simeq |\psi_n^{(0)}|^2$, which is independent of N and of j . Hence $\mathcal{P}_N^{(j)}(n)$ has the limit distribution

$$\mathcal{P}(n) = |\psi_n^{(0)}|^2, \quad n = 0, 1, \dots, K, \quad N \rightarrow \infty. \quad (3.14)$$

The normalization of $\psi^{(0)}$ implies that of \mathcal{P} and *vice versa*.

Equations (3.12) and (3.14), therefore, relate the quantities of physical interest $\langle n \rangle$, $\langle \ell \rangle$, and $\mathcal{P}(n)$, to the largest eigenvalue λ_0 and its eigenvector $\psi^{(0)}$. To find λ_0 and $\psi^{(0)}$ we will have recourse to numerical techniques in section 3.4. Before applying these, however, we present in section 3.2 a heuristic argument that will establish the boundary delimiting the equilibrium regime (regime I) in the $z\omega$ plane, and in section 3.3 some Monte Carlo results that illustrate the equilibrium behavior of the polymers.

3.2 Heuristics: Phase diagram

We expect that for small enough z the average polymer length and other physical quantities will have finite values that tend to well-defined limits when the cutoff K is sent to infinity. But we also expect that for large enough z the typical polymer will be as long as is allowed by the cutoff K . Hence for $K \rightarrow \infty$ there must be in the $z\omega$ plane a phase boundary $z = z_c(\omega)$ between these two regimes. We present now a heuristic argument that determines this phase boundary by balancing entropy against energy.

In the trivial interactionless case, $\omega = 1$, when the length of a polymer is increased from n to n' , its Boltzmann weight acquires a factor $(2z)^{n'-n}$, the entropic coefficient 2 being due to the two types of monomers that are possible at each unit length increase. This establishes that for $z < \frac{1}{2}$ the distribution of the polymer length n will decay exponentially, whereas for $z > \frac{1}{2}$ the polymers will grow until stopped by the cutoff K . The heavy dot on the z axis in figure 2 separates the two regimes.

We now consider how this picture is changed in the case of an overlap weight $\omega > 1$. Let us first suppose that all polymers have a length of order n where n is large. If a polymer of length n is forced to be identical to a neighboring polymer of at least the same length, its entropy change is $-n \log 2$ (it goes down) and its energy change is $-\epsilon n$ (it also goes down). Hence its Boltzmann weight acquires a factor $(\omega/2)^n$. Making neighboring polymers *of given lengths* identical is favorable when this factor exceeds unity, that is,

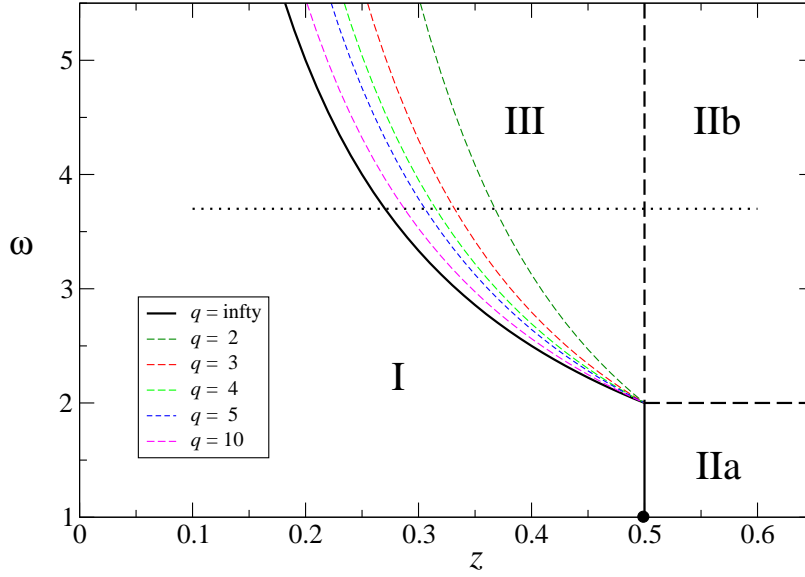


Figure 2: Phase diagram in the $z\omega$ plane. In the limit of cutoff $K \rightarrow \infty$ there appear three regimes, separated by solid or dashed black lines. In regime I a true equilibrium state exists with a finite average polymer length $\langle n \rangle$; in regimes II and III the equilibrium is unstable and the polymer length may grow without limit. In regime II ($z > \frac{1}{2}$) this unbounded growth is due to the sole pressure of the monomer fugacity z ; the distinction between IIa and IIb is briefly discussed at the end of section 4.3. In regime III the unbounded growth is due to the *combined* effect of the monomer fugacity z *and* the polymer-polymer interaction ω ; this is the analog of autocatalytic self-replication in other models. The curved part of the boundary between regimes I and III is given by $z\omega = 1$. The colored dashed curves are given by $\omega = (2z^q)^{-1/(q-1)}$, for $q = 2, 3, 4, \dots$ and are interpreted in section 4.2. The dot on the z axis indicates the phase transition point in the trivial interactionless case, $\omega = 1$. The simulations in this work are at fixed $\omega = 3.7$ and for varying z , that is, along the thin dotted horizontal line.

when $\omega > 2$. Next we determine under which conditions the polymers will satisfy the prerequisite of having large lengths. Suppose a site is occupied by a long polymer of length n . Placing on the site next to it an identical polymer will multiply the Boltzmann weight by a factor $z^n \omega^n$. Hence for $z\omega > 1$ it will be favorable for n to become large.

These arguments together define the equilibrium regime (regime I) of the phase diagram: it is located to the left of the boundary $z_c(\omega) = \min(\frac{1}{2}, \omega^{-1})$, shown as a solid black line in figure 2 and consisting of a straight vertical segment and a curved part. When this boundary is approached from the left, the equilibrium average $\langle n \rangle$ diverges. There is, however, a difference between entering regime IIa and entering regime III. When the boundary with regime IIa is approached, $\langle \ell \rangle$ remains finite: the polymers can grow to infinity under

the sole influence of the monomer fugacity z and their entropy gain associated with having greater length. By contrast, when the boundary with regime III is approached, the argument of the preceding paragraph indicates that $\langle \ell \rangle$ diverges along with $\langle n \rangle$. We identify regime III as the regime of greatest interest: it is characterized by interaction mediated unlimited polymer growth. In this regime the interaction between identical neighboring polymers produces consequences similar to the autocatalytic effects incorporated in other models [1, 3, 4, 5]. We will analyze this phenomenon in detail in section 4 by investigating the behavior of this model along the dotted line in figure 2, that is, as a function of z at a fixed value of ω .

In spite of the heuristic nature of these arguments, we believe on the basis of what will follow below that the results so obtained are exact.

3.3 Monte Carlo simulation in equilibrium

We have performed standard heat bath Monte Carlo dynamics, allowing each polymer P_i to change its length by addition or suppression of a single monomer at a time, attributable to exchange with a reservoir of the two types of monomers. In regime I this dynamics is guaranteed to reproduce the equilibrium statistics of the model.

We carried out a simulation at an arbitrarily fixed value $\omega = 3.7$ while choosing $z = 0.26900$ closely below the (at this stage still presumed) critical point $z_c = 1/\omega = 0.270270\dots$. Figure 3 shows a typical equilibrium configuration of the polymer lengths n_i as a function of the site index i for a portion of a larger system. It also shows the nearest-neighbor overlaps $\ell_{i,i+1}$. The strong correlation between these two “profiles” shows that in order for large fluctuations to arise there has to be sufficient overlap between neighboring polymer pairs, in agreement with the heuristic argument of the preceding subsection.

The profiles are only projections of the full phase space configuration in that they hide the underlying structure of the polymers as sequences of two types of monomers. As an illustration of the monomer structure we represent in figure 4 the specific monomer sequences of the polymers on sites $i = 635$ through $i = 666$ corresponding to figure 3. Figure 4 shows that there are dips in the overlap that coincide with dips in the polymer lengths.

We will be especially interested in the approach of the critical point, $z = z_c$. Figure 5 shows as open black circles the Monte Carlo results for $\langle n \rangle$ as a function of $z_c - z$ on a lattice of $N = 960$ sites. These data result from averaging over a succession of 10^{10} attempted moves, that is, over 1.04×10^7 sweeps through the lattice. They have error bars less than their symbol size. We consider them as preliminary to the transfer matrix results for $\langle n \rangle$, to be discussed in the next subsection.

3.4 Transfer matrix based numerical analysis

We have not been able to diagonalize the reduced transfer matrix \tilde{T} of equation (3.8) analytically. However, exploiting it numerically is easy. At the same fixed value $\omega = 3.7$ of the interaction we have studied the average polymer length $\langle n \rangle$ and average overlap $\langle \ell \rangle$ for varying monomer fugacity z , that is, along the thin dotted line in figure 2. We proceeded by numerically finding the largest eigenvalue λ_0 and corresponding eigenvector $\psi^{(0)}$ of \tilde{T} and we obtained $\langle n \rangle$ and $\langle \ell \rangle$ from it by numerical differentiation. At each value of z the procedure was carried out for increasing values of the cutoff until convergence was obtained.

A critical point appears at a location fully compatible with the heuristic prediction $z = z_c = \omega^{-1} = 0.270270\dots$. We have therefore plotted our numerically exact results in figure 5 as a function of $z_c - z$. Our data point closest to z_c is at $z = 0.27026$; it has $\langle n \rangle = 99.6$ and required a cutoff $K \gtrsim 300$. This figure shows that as z_c is approached, the data points follow asymptotically a straight line, thereby lending support to our assumed value of z_c . The figure strongly suggests, furthermore, that $\langle \ell \rangle$ has the same asymptote as $\langle n \rangle$. This means that upon approach of criticality neighboring polymers are correlated over almost their full length: they can only grow coherently.

The log-log plot of figure 5 implies that

$$\langle n \rangle \sim (z_c - z)^{-\alpha}, \quad z_c - z \rightarrow 0. \quad (3.15)$$

If one considers likely that the exponent is a simple fraction, then the figure is a strong indication that $\alpha = 1/3$. An explanation of this exponent value appears if one views the succession of polymer lengths n_1, n_2, \dots, n_N as the height variables of a one-dimensional interface near a wall (the latter represented by all $n_i = 0$) in a potential that increases with the distance from the wall. In such models the interface width is known to diverge with the $1/3$ power of the inverse potential strength [8]. We elaborate on this approximate analogy in Appendix A.

We have, next, studied the polymer length distribution $\mathcal{P}(n)$. As expected, this distribution is concentrated near the origin $n = 0$ for $z < z_c$ and near the cutoff $n = K$ for $z > z_c$. Its behavior exactly at the critical point $z = z_c$ is interesting. We have determined it from the largest eigenvector $\psi^{(0)}$ of the transfer matrix with the aid of equation (3.14) for different values of the cutoff K . A data collapse is obtained by the scaling

$$\mathcal{P}(n) = \frac{1}{K} \Pi\left(\frac{n}{K}\right) \quad (3.16)$$

and shown in figure 6. We observed that even for very small nonzero $|z - z_c|$ the curve $\Pi(x)$ develops discontinuities of slope near both ends of its interval.

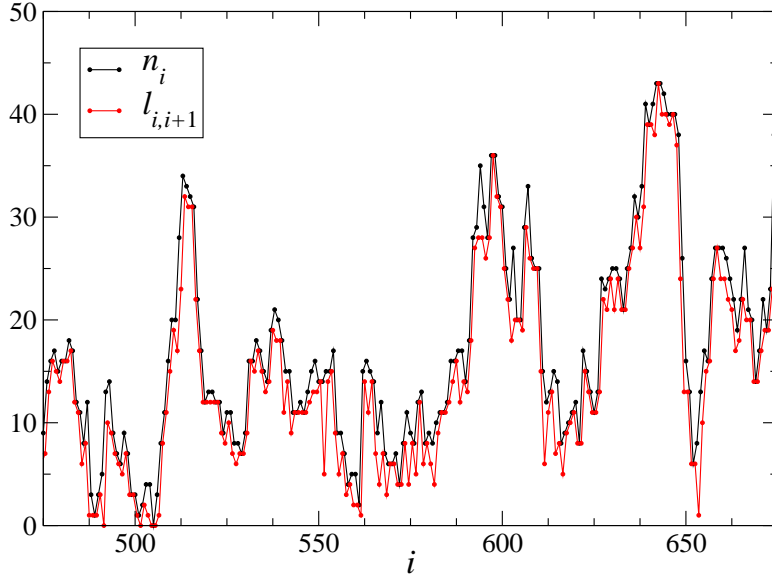


Figure 3: A typical local equilibrium configuration of the n_i and $\ell_{i,i+1}$ at overlap weight $\omega = 3.7$ and for a monomer fugacity $z = 0.26900$, below the critical point $z_c = 0.27027$. The $\ell_{i,i+1}$ have been plotted at the half-integer coordinates $i + \frac{1}{2}$. There is very strong correlation between the $\ell_{i,i+1}$ and their neighboring n_i . For an initial configuration without polymers (all $n_i = 0$), the equilibration time is of the order of $t = 5 \times 10^5$ sweeps through the lattice.

We consider this as another confirmation of the exactness of the location of the critical point at $z_c = 1/\omega$.

As a consequence of equation (3.16) the average polymer length at the critical point is proportional to the cutoff,

$$\langle n \rangle_c \simeq aK, \quad K \rightarrow \infty, \quad (3.17)$$

with an estimated coefficient $a \equiv \int_0^1 dx x \Pi(x) \approx 0.639$.

4 Time evolution

4.1 Cutoff and time evolution

Once we set $K = \infty$ there exists in regimes II and III neither an equilibrium state nor a nonequilibrium steady state. When starting with a collection of polymers of finite length (or, for simplicity, in the state of zero polymers, $n_i = 0$ for all $i = 1, 2, \dots, N$), we may ask what happens under the Monte Carlo dynamics in these unstable regimes. We certainly expect formation of polymers of ever increasing length, and it is of interest to investigate the asymptotic behavior of this process. There is no easy way to analytically

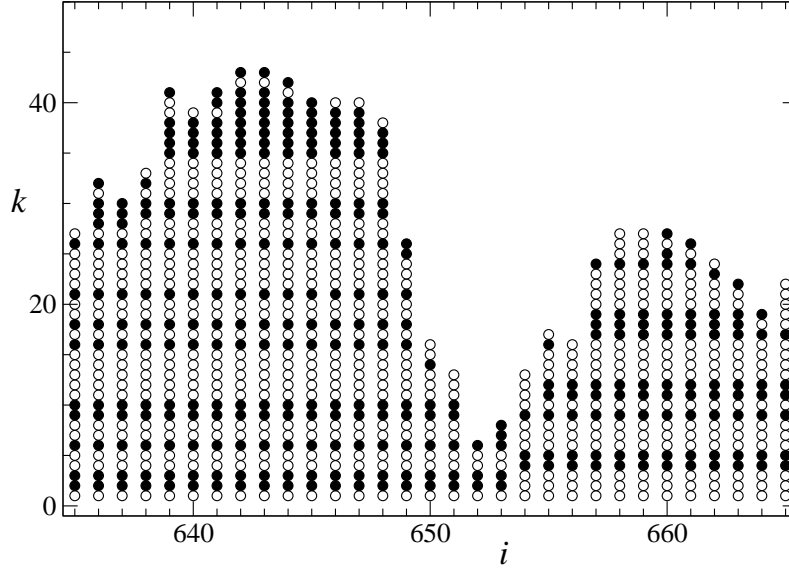


Figure 4: Lattice representation of the full monomer sequences of the polymers on sites 635 through 665 for the same configuration that led to figure 3. Site (i, k) in this figure is marked by an open or a closed circle for monomer variable $s_{ik} = 1$ or $s_{ik} = -1$, respectively. The overlaps $\ell_{i,i+1}$ may be read off from this representation. In the figure they attain a minimum value equal to 1 between the sites $i = 653$ and $i + 1 = 654$.

answer these questions and we will therefore have recourse to simulation and heuristic arguments.

4.2 Heuristics: Growth in the unstable regime

We first present a heuristic argument that tries to describe the time evolution in regime III. By a “block” we will mean an interval of sites occupied by sufficiently long strongly overlapping polymers (strong overlap meaning that $\ell_{i,i+1}$ is typically close to its maximum possible value $\min(n_i, n_{i+1})$), whereas the overlap with the two polymers on the sites just outside the interval is negligible.

We consider an idealized block of q sites $i + 1, i + 2, \dots, i + q$ occupied by q identical polymers of length n , so that all nearest neighbor overlaps are also equal to n . Let moreover the polymers at the end sites of this interval have zero overlap with their neighbors just outside the interval. Suppose now that we increase each of the q polymers by a single link, the same one on all q sites. This will multiply the weight of this set of polymers by the factor $2z^q\omega^{q-1}$, the coefficient 2 being due to the two possible choices for the new

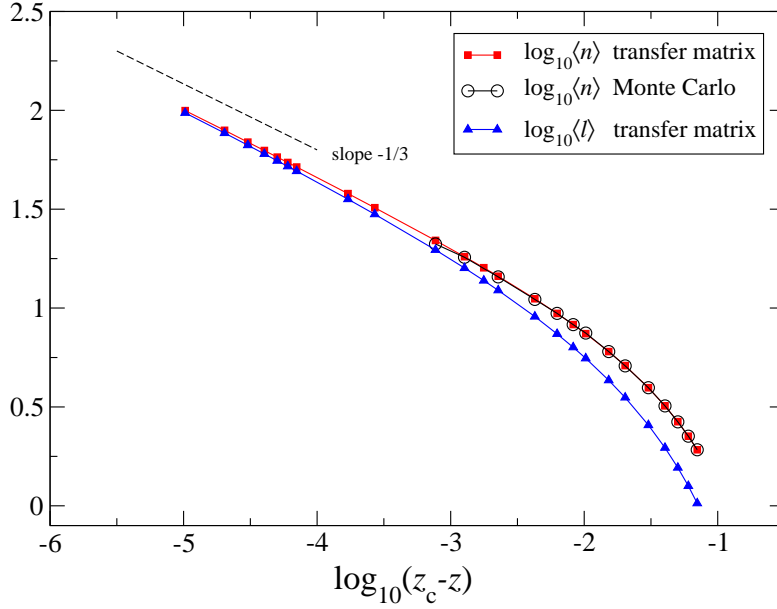


Figure 5: Divergence of $\langle n \rangle$ and $\langle \ell \rangle$ as the monomer fugacity z approaches the critical point z_c from below at overlap weight $\omega = 3.7$. This log-log plot, together with the arguments presented in the text, strongly suggests the asymptotic behavior $\langle n \rangle \sim \langle \ell \rangle \sim (z_c - z)^{-1/3}$. The Monte Carlo data were obtained as described in section 3.3, the transfer matrix results as in section 3.4. The two methods fully agree, the latter being clearly more powerful.

link. This factor is larger than unity when the block size² q is larger than a “correlation length” ξ_{\min} given by

$$\xi_{\min}(z, \omega) \equiv \frac{\log(\omega/2)}{\log(z\omega)}. \quad (4.1)$$

For $q > \xi_{\min}$ the polymers on this interval can grow collectively without limit; for $q < \xi_{\min}$ no such growth is possible. Hence ξ_{\min} is a dynamically required minimum correlation length.

For $z_c < z < \frac{1}{2}$ the correlation length ξ_{\min} goes down smoothly from infinity to unity. Based on equation (4.1) we may in the phase diagram construct the curves $\xi_{\min} = q$, which leads to the set of curves

$$\omega = (2z^q)^{-1/(q-1)}, \quad q = 1, 2, \dots, \quad (4.2)$$

represented by colored dashed lines in figure 2. According to the argument above, in the subregion of regime III between the curves labeled $q - 1$ and q the average polymer length in a block can grow only for a block size at least

²Our terminology will be to speak of the *size* of a block, as opposed to the *lengths* of the polymers that constitute it.

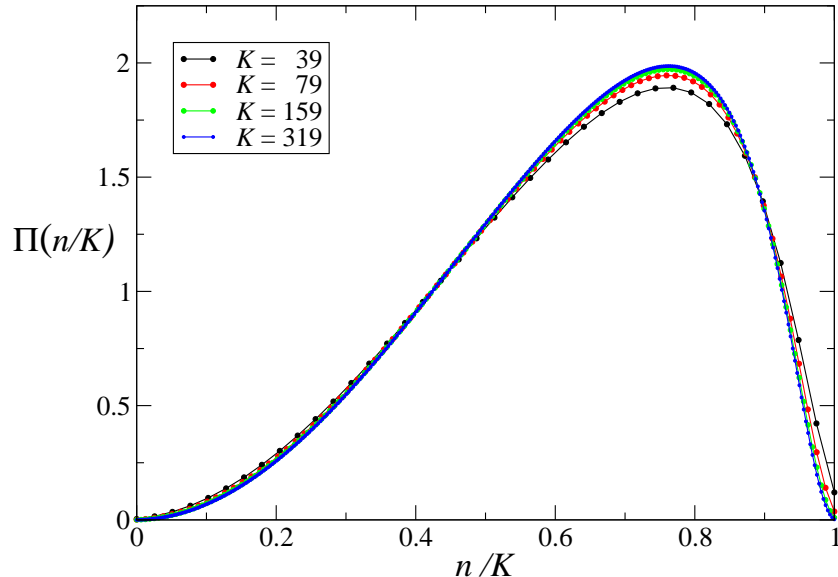


Figure 6: Critical probability distribution $\Pi(n/K)$ of the scaled polymer length n/K at $\omega = 3.7$ and for different values of the cutoff length K . As K increases, the scaled distribution appears to tend to a limit.

equal to q . The vertical black dashed line is the curve for $q = 1$. To its right the polymers no longer need their interaction to grow and a growing polymer will eventually follow its own unique path in the binary tree.

In the real system juxtaposed blocks will interact, which augments the approximate nature of the preceding argument. We expect, nevertheless, to see the effects discussed above at least qualitatively in the Monte Carlo simulations.

4.3 Simulation results

We have simulated the polymer growth in regime III, continuing along the same line $\omega = 3.7$ (see figure 2) that was studied in section 3.4, and starting from an initial state without any polymers. Our results involve lattices of different sizes N and in each case the time variable t will stand for the physical time, that is, the average number of update attempts per lattice site. We imposed periodic boundary conditions, mainly in order to obtain better estimates of bulk quantities, and chose the cutoff large enough (often $K = 10\,000$) so that it was never attained during the time interval of the simulation.

Our principal finding is that above the critical point, $z > z_c$, there occurs a dynamical symmetry breaking: the system forms blocks of finite size that, at least initially, become larger due to a coarsening process. As soon as a block

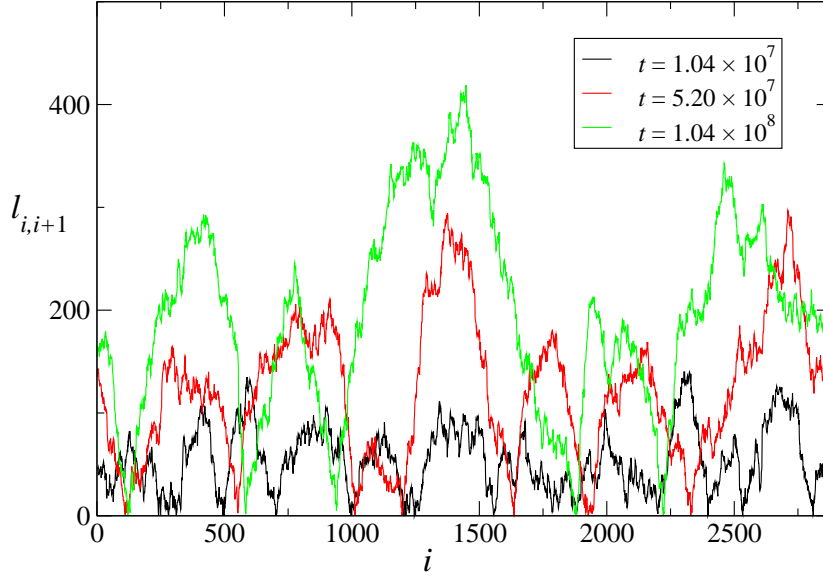


Figure 7: The overlaps $\ell_{i,i+1}$ as a function of the lattice site coordinate i at overlap weight $\omega = 3.7$ and monomer fugacity $z = 0.27040$, that is, just above the critical point $z_c = 0.27027$. The profile is for a system of $N = 2880$ sites at three different times. The correlation length of the profile is seen to grow with time.

size exceeds the minimum required value $\xi_{\min}(z, \omega)$, the average polymer length in the block (the “block profile”) starts growing quasi-independently of its neighboring blocks. Under the biological interpretation such a block represents a set of self-replicating molecules of a selected species. We will now show this in detail.

In figure 7 the monomer fugacity $z = 0.27040$ is just above the critical point $z_c = 0.27027$. This figure shows the profile of the overlaps $\ell_{i,i+1}$ as a function of the lattice site coordinate i in a system of $N = 2880$ sites and for three different times.³ One clearly distinguishes blocks in the above defined sense: large size intervals of considerable overlap are separated by narrow, almost point-like, intervals of close-to-zero overlap.

As time goes on two things happen, namely (i) the amplitude of the profile fluctuations increases; and (ii) there is a coarsening causing the typical block size, that we will denote by $\xi(t)$, to increase with time. We will also refer to $\xi(t)$ as the system’s time dependent *correlation length*. This length $\xi(t)$ should be compared with the value $\xi_{\min} = 1282$, obtained from equation (4.1). In figure 7 the simulation time $t = 1.04 \times 10^8$ is not long enough for $\xi(t)$ to reach this minimum value. As a consequence the three curves are still in what should be called the critical regime: each of them resembles the

³Just as is figure 3, the profiles of the n_i very nearly coincide with those of the $\ell_{i,i+1}$. We therefore do not show them in figure 7.

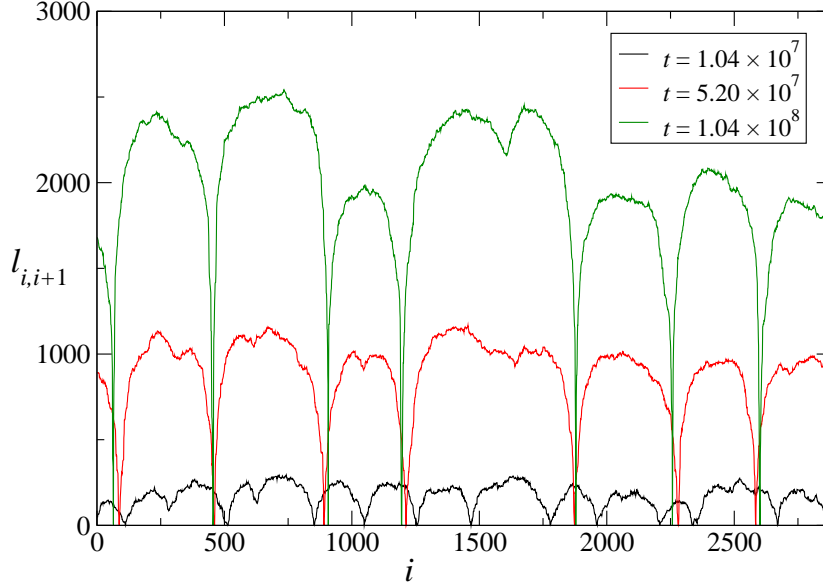


Figure 8: The overlaps $\ell_{i,i+1}$ at overlap weight $\omega = 3.7$ and monomer fugacity $z = 0.27100$ in a system of 2880 sites at three different times. Comparison of the profiles at the later two times shows that the growth of the typical block size has come to a standstill.

equilibrium profile of figure 3. At these values of z and ω longer simulation for a larger lattice would be needed to take the system out of the critical region.

In figure 8 the overlap weight still has the same value $\omega = 3.7$ but the monomer fugacity $z = 0.27100$ is further above the critical point $z_c = 0.27027$ and the growth of the profile, shown at the same three times as in figure 7, is much faster. The black curve, taken at the earliest time $t = 1.04 \times 10^7$, has twelve clearly marked minima at or close to zero, which corresponds to a correlation length that we may roughly estimate as $\xi(t) = 2880/12 = 240$. At the later time $t = 5.20 \times 10^7$ the red curve shows that the system has coarsened to only seven such minima, whence a correlation length that has gone up to $\xi(t) = 2880/7 = 411$. However, at still later times, the green curve shows that the coarsening appears to have stopped, with a correlation length frozen⁴ at the asymptotic value $\xi(\infty) = 411$. For comparison, equation (4.1) gives $\xi_{\min} = 228$ for this pair (z, ω) . We observe here that in the actual system the block sizes are distributed in an interval that extends roughly from ξ_{\min} to $2\xi_{\min}$. This is easily understood: blocks smaller than ξ_{\min} cannot grow and blocks larger than $2\xi_{\min}$ gain entropy by splitting up into two blocks both

⁴We cannot exclude mathematically that for much later times the coarsening still continues at some exponentially small rate; however, for all practical purposes it has come to an absolute stop.

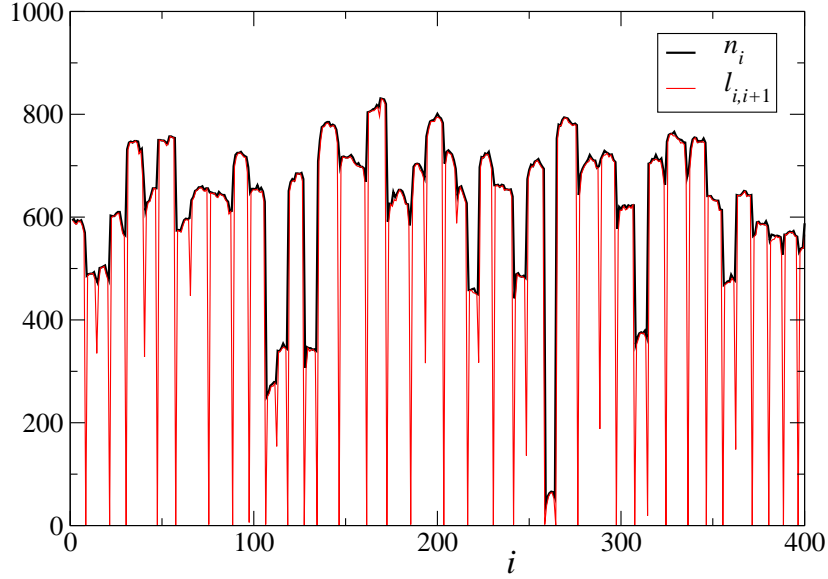


Figure 9: The polymer lengths n_i (black) and overlaps $\ell_{i,i+1}$ (red) at overlap weight $\omega = 3.7$ and for monomer fugacity $z = 0.3$ in a system of $N = 400$ sites, as observed at time $t = 2.5 \times 10^5$.

larger than ξ_{\min} .

On the asymptotic time scale the profiles in the different block profiles appear to grow linearly with time. Growth speeds are somewhat block size dependent, being larger for the larger blocks. The largest size block in figure 8, namely the one extending between approximately $i = 1200$ and $i = 1900$, shows a tendency to split in two, which causes its growth to somewhat slow down.

Figure 9 is still for $\omega = 3.7$ but was obtained for monomer fugacity $z = 0.3$, well above the critical point $z_c = 0.27027$. For this pair (z, ω) equation (4.1) yields $\xi_{\min} = 5.9$. The polymer growth is much faster than near the critical point and the data were taken at time $t = 2.5 \times 10^5$.

The red curve represents the $\ell_{i,i+1}$ profile; in this figure we have again shown the n_i profile, which differs from the $\ell_{i,i+1}$ near the block boundaries. Several of the blocks are subject to splitting attempts, which makes the determination of the typical block size somewhat ambiguous. By taking into account that the $\ell_{i,i+1}$ profile has about 33 zeros or near-zeros we arrive at the estimate $\xi(\infty) = 400/33 = 12.1$. The actual block sizes are again distributed in a range going from ξ_{\min} to about $3\xi_{\min}$, again confirming the role played by ξ_{\min} : growing blocks respect this minimum size condition. The typical block profile grows again linearly with time. Clearly some of the smaller blocks, of sizes around or below the minimum size, do not grow well.

For completeness we briefly discuss regimes IIa and IIb. When z is further increased, the dynamically required minimum correlation length ξ_{\min} crosses unity at $z = \frac{1}{2}$ and the system enters regime IIb. For $z > \frac{1}{2}$ each polymer can grow independently of its neighbors. This is “disordered growth” in the sense that, contrary to what happens in regime III, no specific polymer types are selected and dominate. In regime IIb blocks of two (or more rarely a few) polymers are observed to grow coherently until at some point in time they break up, after which each polymer grows independently of its neighbors. This entails that $\langle \ell \rangle$ saturates at a finite value: the $\ell_{i,i+1}$ decouple from the n_i . The typical break-up time increases with ω and decreases with z .

The dynamical scenario in regime IIa is qualitatively the same as in IIb. The two regimes distinguish themselves by the behavior of the limit $K \rightarrow \infty$: in regime IIb this limit is accompanied by both $\langle n \rangle \rightarrow \infty$ and $\langle \ell \rangle \rightarrow \infty$, whereas in regime IIa we have $\langle n \rangle \rightarrow \infty$ but $\langle \ell \rangle$ remains finite. The observed fact that dynamically $\langle \ell \rangle$ remains finite in both regimes shows that the limits $K \rightarrow \infty$ and $t \rightarrow \infty$ do not commute.

5 Discussion

Biological evolution necessarily involves a transition from prelife to life. Within the context of simplified models “prelife” is considered as characterized by the spontaneous growth of long polymers due to the addition of single monomers one at a time, whereas “life” is characterized by the self-replication, or autocatalytic polymerization, of certain polymer species. Models of interest are those in which a tuning of parameters may take us from a prelife phase to a life phase. After having in the preceding sections exposed and analyzed our model we will discuss here some of its similarities and differences with, specifically, the work of Wu and Higgs [3, 4] and of Chen and Nowak [5].

Wu and Higgs [3] study a system of polymers of which they ignore the nucleotide sequences, keeping track only of their lengths. They formulate a set of coupled rate equations for the concentrations of polymers of given length. A nonlinear term in the equations represents the autocatalytic effect responsible for self-replication; it becomes operative only once spontaneous polymerization in the prelife state has led to the appearance of polymers exceeding a fixed threshold length. The rate equations then have two stable stationary states of which the one with the lower (higher) concentration of long polymers is interpreted as the “prelife” (“life”) state.

In a subsequent two-dimensional non-well-mixed version of their model Wu and Higgs [4] study spatial fluctuations. They find that the prelife state is metastable and that the appearance of life is a one-time local stochastic

event. It is, essentially, analogous to the process, well-known in statistical physics, of crossing a nucleation barrier in the Ising model.

Ignoring the specificity of the monomer sequences precludes observing the phenomenon of selection. The work by Chen and Nowak [5] does describe such a selection. These authors consider a reservoir of two types of monomers from which an arbitrary number of polymer species $p = (n, p^n)$ may grow,⁵ that is, their phase space has the same binary tree structure as ours. In order to represent the complexity of the actual chemical kinetics, the authors introduce randomly fixed spontaneous growth rates, controlled by a parameter s , and randomly fixed replication rates, controlled by a parameter r , the latter rates being intended to mimic the autocatalytic effects. Chen and Nowak then set up rate equations for the time evolution of the species concentrations $x_p(t)$. All species grow and replicate independently of one another, apart from a collective scaling imposed by a depletion term that keeps the total concentration fixed.

Chen and Nowak’s model has polymerization but no depolymerization reactions. There is, therefore, no such thing as detailed balancing, nor a thermodynamical equilibrium. The system evolves towards a stationary state⁶ which, depending on the value of the replication parameter r , may either contain a mix of species of different lengths and compositions, or be strongly dominated by the abundance of a single species, selected by the random landscape. Between the two regimes there is no sharply defined phase transition point in the sense of statistical mechanics; however, on the r axis a narrow “critical interval” separates prelife from life.

By comparison, our model provides a description in terms not of concentrations but of individual polymers. It is governed not by rate equations but by a multidimensional master equation, implemented by Monte Carlo dynamics. Our two parameters, the monomer fugacity z and the weight factor ω that represents the interaction strength, play very approximately the same role as the parameters r and s , respectively, in reference [5].

The most distinguishing feature of the present model is the presence of a polymer-polymer interaction, albeit one of a very elementary kind, which expresses that in order for one long polymer to catalytically favor the creation of another one, their two monomer sequences have to be in a precise relation. A consequence of this interaction is that polymer growth is possible only as a collective phenomenon. It leads to the growth of a limited set of preferred species, the selection being determined by a random dynamical symmetry breaking. This selection, which occurs in a regime of the $z\omega$ plane that we

⁵The notation here is as in section 2: p^n is a sequence of n binary variables.

⁶ The authors use the term “equilibrium state” for what in statistical physics is usually called a (nonequilibrium) stationary state.

identified as regime III, illustrates a theme stated in reference [5], namely that prelife allows coexistence of many species, but that life leads to competitive exclusion.

The main conclusion of this work is that selection of certain species at the cost of others may be the result of interaction between species; and that a random parameter landscape, even though chemically realistic, is not a necessary ingredient. We believe we have provided a complementary way to look at the questions studied in references [1, 3, 4, 5] and hope that this model, or future variants of it, will be of interest to statistical physicists.

A further point deserves mention. The polymers in this work grow without limit. It would be easy to introduce a smooth cutoff by including a depletion process. We consider, however, this infinite growth as the germ of open-endedness that in later work begs to be implemented by cooperative events of greater complexity between the polymers.

6 Conclusion

The transition from prelife to life, that is, from the prebiotic soup to an environment dominated by specific self-replicating long polymers, is an extremely complicated question. It has nevertheless led to a few very simple models in mathematical biology. These in turn have inspired us to construct a toy model meant to be of interest to statistical physicists.

In this model, each site of a one-dimensional lattice is occupied by a polymer, that is, a binary sequence of monomers of variable length. The system evolves in time by addition or suppression of single monomers. Its one-dimensional structure, certainly artificial, has served us to check the Monte Carlo data against analytic results.

The model has an equilibrium phase, in the sense of statistical mechanics, and a “phase,” in a more general sense, that is neither stationary nor evolves towards a stationary one, and is dominated by specific selected polymers. We view this latter phase as the rudimentary precursor of an open-endedly evolving system. The existence of this “life phase” is not due to an explicitly incorporated autocatalytic term as in earlier work [3, 4, 5], but is the consequence of an interaction at the monomer level between different polymer species. The prelife-to-life transition is a transition between these two phases.

We have not explored all aspects of this model and many further questions could be asked. Other models of the same kind also seem worthy of being developed and studied. Preliminary results by ourselves indicate that a mean-field (“well-mixed”) version of this model has essentially the same properties as those found here in one dimension. We leave the study of these and other extensions to future work.

A Appendix: The $\{n_i\}$ viewed as an interface

We consider in this Appendix the variable n_i , for $i = 1, 2, \dots, N$, as the height at site i of a one-dimensional interface. The condition $n_i \geq 0$ represents a “hard wall.” A general expression for the energy $E_{\text{int}}\{n_i\}$ associated with an interface configuration $\{n_i\}$ is

$$E_{\text{int}} = \sum_{i=1}^N H(n_i) + \sum_{i=1}^{N-1} V(n_i, n_{i+1}) \quad (\text{A.1})$$

This expression was studied in reference [8] for several different cases. The authors investigated in particular the linearly increasing on-site potential $H(n_i) = gn_i$ and the “SOS” interaction $V(n_i, n_{i+1}) = 2K|n_i - n_{i+1}|$, in which g is the “gravitational constant” and $2K$ the “elastic” energy. They found that for $g \rightarrow 0$ the interface width diverges as $\langle n \rangle \sim g^{-1/3}$.

In the present work there is an effective interaction associated with each pair of neighboring variables $n_i \equiv n$ and $n_{i+1} \equiv m$, mediated by the traced-out overlap $\ell_{i,i+1}$ and explicitly given by

$$E_{\text{int}} = \sum_i \log \tilde{T}_{n_i, n_{i+1}}, \quad (\text{A.2})$$

where we ignore boundary terms. When (3.8) and (3.6) are substituted in (A.2) and when we take $\nu \equiv \min(m, n)$ large, we find the expansion

$$\log \tilde{T}_{nm} = \nu \log z\omega + \frac{1}{2}|n - m| \log 2z + \text{cst} + \mathcal{O}((2/\omega)^\nu), \quad \nu \rightarrow \infty, \quad (\text{A.3})$$

valid for $\omega > 2$. The coefficient $\frac{1}{2} \log 2z$ of the elastic term keeps a finite value when $z \rightarrow z_c = \omega^{-1}$. It multiplies $|n - m|$, and hence this term is identical to the SOS interaction of reference [8]. The coefficient $\log z\omega$ of the potential term vanishes as $\sim (z - z_c)\omega$ for $z \rightarrow z_c$ and plays the role of the limit $g \rightarrow 0$ in reference [8]. It multiplies, however, the minimum $\nu = \min(m, n)$ rather than the symmetric sum $\frac{1}{2}(m + n)$. This difference, plus the fact that we have expanded for large ν , makes our model different from that of reference [8]. We may nevertheless speculate that with respect to their critical behavior these two models are in the same universality class, which explains the exponent $\alpha = 1/3$ found in the simulation of section 3.4.

References

- [1] F.J. Dyson, *J. Mol. Evolution* **18** (1982) 344.
- [2] H.A. Kramers, *Physica* **7** (1940) 284.
- [3] M. Wu and P.G. Higgs, *J. Mol. Evolution* **69** (2009) 541.

- [4] M. Wu and P.G. Higgs, *Biology Direct* **7**:42 (2012).
- [5] I.A. Chen and M.A. Nowak, *Accounts of Chemical Research* **45** (2012) 2088.
- [6] M.A. Bedaux, in: A.S. Wu (ed.), *Proceedings of the 1999 Genetic and Evolutionary Computation Conference Workdhop Program*, pp.20-23. Morgan Kaufmann, San Francisco.
- [7] W. Banzhaf and L. Yamamoto, *Artificial Chemistries* (MIT Press, Cambridge, Massachusetts, 2015).
- [8] J.M.J. van Leeuwen and H.J. Hilhorst, *Physica* **107A** (1981) 319.